



Investigations of approximate expressions for the transit duration

David M. Kipping^{1,2★}

¹Harvard-Smithsonian Center for Astrophysics, 60 Garden St., Cambridge, MA 02138, USA

²Department of Physics and Astronomy, University College London, Gower Street, London WC1E 6BT

Accepted 2010 April 21. Received 2010 April 21; in original form 2010 January 22

ABSTRACT

In this work, we investigate the accuracy of various approximate expressions for the transit duration of a detached binary against the exact solution, found through solving a quartic equation. Additionally, a new concise approximation is derived, which offers more accurate results than those currently in the literature. Numerical simulations are performed to test the accuracy of the various expressions. We find that our proposed expression yields a >200 per cent improvement in accuracy relative to the most previously employed expression.

We derive a new set of equations for retrieving the light-curve parameters and consider the effect of falsely using circular expressions for eccentric orbits, with particularly important consequences for transit surveys. The new expression also allows us to propose a new light-curve fitting parameter set, which minimizes the mutual correlations and thus improves computational efficiency. The equation is also readily differentiated to provide analytic expressions for the transit duration variation due to secular variations in the system parameters, for example due to apsidal precession induced by perturbing planets.

Key words: methods: analytical – techniques: photometric – celestial mechanics – eclipses – planetary systems.

1 INTRODUCTION

Transiting exoplanets and eclipsing binaries produce familiar U- and V-shaped light curves with several defining quantities, such as the mid-eclipse time, eclipse depth and duration. Out of these, the transit duration is undoubtedly the most difficult observable to express in terms of the physical parameters of the system. (Kipping 2008, hereafter K08) showed that the duration is found by solving a quartic equation, to which exists a well-known solution. In general, two roots correspond to the primary eclipse and two to the secondary but this correspondence determination has an intricate dependency on the input parameters for which there currently exist no proposed rules. As a consequence, there currently exists no single exact expression for the transit duration.

In many applications, the process of discarding unwanted roots may be performed by a computer, but naturally this can only be accomplished for case-by-case examples. The benefits of a concise, accurate and general expression for the transit duration, as we will refer to it from now on, are manifold. The solution provides lower computation times, deeper insight into the functional dependence of the duration and a decorrelated parameter set for fitting eclipse light curves (see Section 6). Such a solution may also be readily differentiated to investigate the effects of secular and periodic changes in the system (see Section 7). With the changes in

transit duration recently being proposed as a method of detecting additional exoplanets in the system (Miralda-Escudé 2002; Heyl & Gladman 2007) and companion exomoons (Kipping 2009a,b), there is a strong motivation to ensure an accurate, elegant equation is available.

In this work, we will first propose a new approximate expression for the transit duration in Section 2. In Section 3, we will derive two new approximate expressions for the transit duration and discuss others found in the literature; exploring their respective physical assumptions and derivations. In Section 4, we present the results of numerical tests of the various formulae. We find that one of our new proposed expressions offers the greatest accuracy out of the candidates. In Sections 5 and 6, we utilize the new equation to derive mappings between the observable transit durations and the physical model parameters. These mappings may be used to obtain a decorrelated transit light-curve fitting parameter set, which enhances the computational efficiency of Monte Carlo based methods. Finally, in Section 7, we differentiate the favoured solution to predict how the transit duration will change due to apsidal precession, nodal precession, in-fall and eccentricity variation.

2 THE TRANSIT DURATION EQUATION

2.1 Exact solution

Before we begin our investigation, let us first clearly define what we mean by the transit duration. There exist several different

★E-mail: d.kipping@ucl.ac.uk

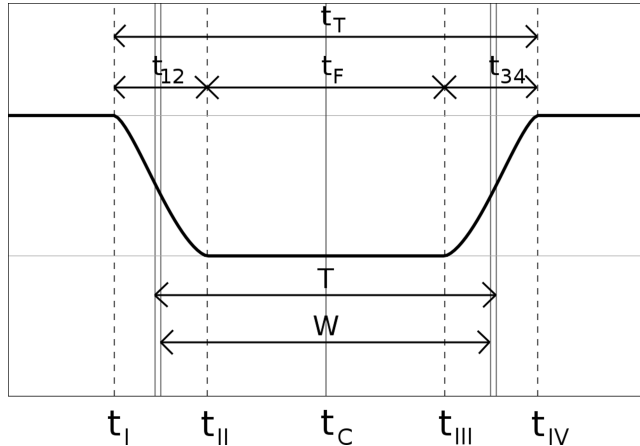


Figure 1. Various definitions of the transit duration are marked on a model transit light curve.

definitions of what constitutes as the transit duration in the exoplanet literature. In Fig. 1, we present a visual comparison of these definitions. There exists at least seven different duration definitions: t_T , t_F , T , W , τ , t_{12} and t_{34} . t_T and t_F are the definitions used by Seager & Mallén-Ornelas (2003, hereafter SMO03) and represent the first to fourth and second to third contact durations, respectively. These can be understood to be the total transit duration and the flat-bottomed transit duration (sometimes confusingly referred to as the full duration). T is the time for a planet to move from its sky-projected centre overlapping with the stellar limb to exiting under the same condition. W is a parameter we define in this work as the average of t_T and t_F which we call the transit width. We note that $T > W$ since when the planet's centre crosses the limb of star, less than one half of the planet's projected surface blocks the light from the star. However, many sources in literature make the approximation $T \simeq W$, which is only true for a trapezoid approximated light curve (a detailed discussion on this is given in Section 6.3). Finally, t_{12} and t_{34} are the ingress and egress durations, respectively, which are often approximated to be equal to one single parameter, τ .

Throughout this paper, we assume that the planet is a black sphere emitting no flux crossing the disc of a perfectly spherical star. The consequences for oblate planets are discussed by Seager & Hui (2002) and for hot planets with significant nightside fluxes in Kipping & Tinetti (2010). We will employ the definition of T for the transit duration. Once the equation for T is known, it is trivial to transmute it to give any of the other definitions provided in Fig. 1.

An exact solution for T , in terms of the true anomaly f , is given by integrating df/dt between f_b and f_a (where we use f to describe true anomaly throughout this paper). Details of the derivation can be found in K08, but to summarize we have

$$T(f_b, f_a) = \left(\frac{P}{2\pi} \frac{1}{\sqrt{1-e^2}} \right) [D(f_b) - D(f_a)], \quad (1)$$

$$D(f) = 2\sqrt{1-e^2} \tan^{-1} \left[\sqrt{\frac{1-e}{1+e}} \tan \frac{f}{2} \right] - \frac{e(1-e^2) \sin f}{1+e \cos f}, \quad (2)$$

$$\begin{aligned} D(f_b) - D(f_a) &= 2\sqrt{1-e^2} \tan^{-1} \left[\frac{\sqrt{1-e^2} \sin f_H}{\cos f_H + e \cos f_M} \right] \\ &\quad - \frac{2e(1-e^2) \sin f_H (e \cos f_H + \cos f_M)}{(1-e^2) \sin^2 f_M + (e \cos f_H + \cos f_M)^2}, \end{aligned} \quad (3)$$

where P is the planetary orbital period, e is the orbital eccentricity, $D(f)$ is the ‘duration function’, $f_M = (f_b + f_a)/2$ and $f_H = (f_b - f_a)/2$. It is clear that two principal terms define D and hence we dub the expressions used here as the ‘two-term’ transit duration equation. At this point, the outstanding problem is solving for f_a and f_b , which are the true anomalies at the contact points.

The K08 solution is derived using Cartesian coordinates, but we consider here a simpler formulation in terms of $\cos(f)$. In order to solve, we must first consider the geometry of the system. As with K08, an ellipse is rotated for argument of pericentre and then orbital inclination. We choose to define our coordinate system with the star at the origin with the $+Z$ -axis pointing at the observer. We also choose to align the $+X$ -axis towards the ascending node of the planetary orbit, which ensures that the longitude of the ascending node satisfies $\Omega = 0$ and the longitude of pericentre (of the planetary orbit) is equal to the argument of the pericentre ($\varpi = \omega$). In such a coordinate system, we may write the sky-projected planet–star separation (in units of stellar radii):

$$S(f) = a_R \frac{1-e^2}{1+e \cos f} \sqrt{1-\sin^2 i \sin^2(\omega+f)}, \quad (4)$$

where a_R is the semimajor axis in units of stellar radii (a/R_*) and i is the orbital inclination. The two contact points occur when S is equal to unity. For a body which undergoes both primary and secondary transit, there must be at least four solutions, which already is an indication of a quartic. If we let $c = \cos f$ and rearrange (4) in terms of purely terms in c , we obtain the following quartic equation:

$$0 = Q_0 + Q_1 c + Q_2 c^2 + Q_3 c^3 + Q_4 c^4, \quad (5)$$

$$Q_0 = (\csc^2 i + \Lambda^2(\cos^2 \omega - \csc^2 i))^2, \quad (6)$$

$$Q_1 = 4e \csc^2 i (\csc^2 + \Lambda^2(\cos^2 \omega - \cos^2 i)), \quad (7)$$

$$\begin{aligned} Q_2 &= \Lambda^2 \csc^2 i (e^2 + (2\Lambda^2 + e^2 - 2) \cos 2\omega) \\ &\quad + 2e^2 \csc^4 i (3 - \Lambda^2) - 2\Lambda^4 \cos^2 \omega, \end{aligned} \quad (8)$$

$$Q_3 = 4e \csc^2 i (e^2 \csc^2 i - \Lambda^2 \cos 2\omega), \quad (9)$$

$$Q_4 = (\Lambda^2 \cos 2\omega - e^2 \csc^2 i)^2 + \Lambda^4 \sin^2 2\omega, \quad (10)$$

$$\Lambda = a_R(1-e^2). \quad (11)$$

Equation (5) is a quartic equation not satisfying any of the special case quartics which are most easily solved (e.g. a biquadratic). Since we have four roots for $c = \cos f$, there are eight roots in total for f , of which only four are physical. Therefore, it is preferable to always work with $\cos f$ since $D(f)$ may be easily expressed in terms of c as well. Although the solutions of a quartic equation are well known, two of the roots correspond to the primary transit and two to the secondary. The correspondence of which roots relate to which contact points varies with an intricate dependency on the input parameters. Unfortunately, no known rules or relations currently exist for this correspondence and we were unable to find a system either. Consequently, there currently exists no single exact equation for the transit duration.

We note that the problem of finding the duration of an eclipse is not a new one. An equivalent problem is considered in Kopal (1959) for the time taken for a body to move between primary and secondary transit. Kopal (1959) showed that a closed-form expression is possible by assuming $i = 90^\circ$. However, this assumption would be too erroneous for the purposes of finding the duration of a transit event.

2.2 Approximation solutions

In order to avoid the quartic equation, we must make an approximation. A useful approximation we can make is that $\varrho(f) \simeq \varrho_c = \varrho(f=f_c)$, i.e. the planet–star separation is approximately a constant value given by the planet–star separation at mid-transit. Defining the transit impact parameter as $b = a_R \varrho_c \cos i$, it may be shown that the difference between f_b and f_a is given by

$$\sin f_H = \sin \left(\frac{f_b - f_a}{2} \right) \simeq \frac{\sqrt{1 - b^2}}{a_R \varrho_c \sin i}. \quad (12)$$

In addition to (12), we require $(f_a + f_b)/2$. A good approximation would appear to be that $(f_b + f_a)/2 \simeq f_c$, which is the true anomaly at mid-transit. f_c is defined as the point where S is a minimum. Differentiating S with respect to f and solving for f leads to a quartic expression again and thus an exact concise solution remains elusive but a good approximation is given by

$$f_M \simeq f_c \simeq \frac{\pi}{2} - \omega. \quad (13)$$

2.3 Two-term expression

By combining equations (1) and (3) with (12) and (13), we are able to obtain a final expression for the duration, which we dub T_2 ('two-term'). Testing T_2 for the exact solutions for f_M and f_H provided precisely the correct transit duration for all e , as expected. However, we found that using approximate entries for these terms severely limited the precision of the derived equation for large e (the results of numerical tests will be shown later in Section 4).

The source of the problem comes from equation (3) which consists of taking the difference between two terms. Both terms are of comparable magnitude for large e and thus we are obtaining a small term by taking the difference between two large terms. These kinds of expressions are very sensitive to slight errors. In our case, the error is from using approximate entries for f_M and f_H . In this next section, we will consider possible 'one-term expressions' which avoid the problem of taking the difference of two comparable-magnitude terms.

2.4 One-term expression

There are numerous possible methods for finding 'one-term' transit duration expressions. Starting from equation (1), we could consider using the same assumption which we used to derive the approximate true anomalistic duration, Δf ; i.e. the planet–star separation does not change during the transit event. This would yield

$$T_1 = \frac{P}{2\pi} \frac{\varrho_c^2}{\sqrt{1 - e^2}} \Delta f, \quad (14)$$

$$T_1 = \frac{P}{\pi} \frac{\varrho_c^2}{\sqrt{1 - e^2}} \arcsin \left(\frac{\sqrt{1 - a_R^2 \varrho_c^2 \cos^2 i}}{a_R \varrho_c \sin i} \right), \quad (15)$$

where we have used equation (12) for Δf . Another derivation would be to assume the planet takes a tangential orbital velocity and constant orbital separation from the planet, sweeping out an arc of length $r_c \Delta f$. It is trivial to show that this argument will lead to precisely the same expression for T_1 .

3 CURRENT EXPRESSIONS FOR THE TRANSIT DURATION

3.1 Seager & Mallén-Ornelas (2003) equation

For a circular orbit, the task of finding the transit duration is greatly simplified due to the inherent symmetry of the problem and an exact, concise solution is possible, as first presented by SMO03:

$$T_{\text{SMO03}} = \frac{P}{\pi} \arcsin \left(\frac{\sqrt{1 - a_R^2 \cos^2 i}}{a_R \sin i} \right). \quad (16)$$

The physical origin of this expression can be seen as simply multiplying the reciprocal of the planet's tangential orbital velocity (which is a constant for circular orbits), by the distance covered over the swept-out arc, $a \Delta f$:

$$T_{\text{SMO03}} = v^{-1} \Delta d,$$

$$T_{\text{SMO03}} = \left(\frac{P}{2\pi a} \right) (a \Delta f), \quad (17)$$

where we expand the first term as the orbital period divided by the orbital circumference, and the second term as the arc length. It may be shown that

$$\Delta f(e=0) = 2 \arcsin \left(\frac{\sqrt{1 - a_R^2 \cos^2 i}}{a_R \sin i} \right). \quad (18)$$

It can be seen that our approximate expression for Δf , presented in equation (12) is equivalent to equation (18) for circular orbits. It is also worth noting that both T_1 and T_2 can be shown to reduce down to T_{SMO03} for circular orbits.

3.2 Tingley & Sackett (2005) equation

Tingley & Sackett (2005, hereafter TS05) presented expressions for the duration of an eccentric transiting planet, which has been used by numerous authors since (e.g. Ford, Quinn & Veras 2008; Jordán & Bakos 2008). It is also forms the basis of a light-curve parameter fitting set proposed by Bakos et al. (2007). There are two critical assumptions made in the derivation of the TS05 formula. The first of these is that

- (i) the planet–star separation, r , is constant during the planetary transit event and equals r_c .

This is the same assumption made in the derivation of the T_1 equation. Under this assumption, TS05 quote the following expression for T (changing to consistent notation):

$$T_{\text{TS05}} = \frac{r_c \Delta \phi}{v_c}, \quad (19)$$

where TS05 define r_c as the planet–star separation at the moment of mid-transit, v_c as the planet's orbital velocity at the moment of mid-transit and $\Delta \phi$ as 'the eccentric angle between the first and last contacts of transit'. In the standard notation, there is no such parameter defined strictly as the 'eccentric angle' and thus we initially assumed that TS05 were referring to the eccentric anomaly. However, substituting the relevant terms for r_c and v_c gives

$$T_{\text{TS05}} = \frac{P}{2\pi} \frac{\varrho_c^2}{\sqrt{1 - e^2}} \Delta \phi. \quad (20)$$

By comparing (20) to equation (14), it is clear $\Delta \phi = \Delta f$ (also note equation (14) was derived under precisely the same assumptions as that assumed by TS05 at this stage of the derivation). We therefore conclude that the term TS05 refer to as 'eccentric angle' in fact

refers to true anomaly. This is an important point to make because the derivation of the TS05 equation would otherwise be very difficult to understand by those working outside of the field. Continuing the derivation from this point, the second assumption made by TS05 is

(i) the planet–star separation is much greater than the stellar radius, $r \gg R_*$.

Critically, this assumption was not made in the derivation of T_1 or T_2 . Using this assumption, TS05 propose that (replacing $\Delta\phi \rightarrow \Delta f$ to remain consistent with the notations used in this work and replacing $(1 + p) \rightarrow 1$ to refer to T rather than the duration from contact points 1 to 4):

$$\Delta f_{\text{TS05}} = \arcsin \left(2 \frac{\sqrt{1 - a_R^2 \varrho_c^2 \cos^2 i}}{a_R \varrho_c} \right), \quad (21)$$

$$\Delta f_{\text{TS05}} \simeq 2 \frac{\sqrt{1 - a_R^2 \varrho_c^2 \cos^2 i}}{a_R \varrho_c}, \quad (22)$$

where TS05 use equation (22) rather than (21) in the final version of T . Therefore, TS05 effectively make a small-angle approximation for Δf , which is a knock-on effect of assuming $r \gg R_*$. We argue here that losing the arcsin function does not offer any great simplification of the transit duration equation but does lead to an unnecessary source of error in the resultant expression, in particular for close-in orbits, which is common for transits. We also note that even equation (21) exhibits differences to equation (12).

First, inside the arcsin function, the factor of $\csc i$ is missing which is present in both the derivation we presented in equation (12) and the derivation of SMO03 for circular orbits, equation (18). The absence of this term can be understood as a result of the $r \gg R_*$ assumption. As $r \rightarrow \infty$, in order to maintain a transit event, we must have $i \rightarrow (\pi/2)$.

Secondly, the expression we presented for Δf earlier in (12) has the factor of 2 present outside of the arcsin function, whereas TS05 have this factor inside the function. Furthermore, the SMO03 derivation also predicts that the factor of 2 should be outside of the arcsin function and this expression is known to be an exact solution for circular orbits. In a small angle approximation, $\arcsin 2x \simeq 2 \arcsin x$, but we point out that moving the factor of 2 to within the arcsin function seems to serve no purpose except to invite further error into the expression. As a result of these differences, the TS05 expression for T does not reduce down to the original SMO03 equation and is given by

$$T_{\text{TS05}} = \frac{P}{\pi} \frac{\varrho_c}{\sqrt{1 - e^2}} \frac{\sqrt{1 - a_R^2 \varrho_c^2 \cos^2 i}}{a_R}. \quad (23)$$

3.3 Winn (2010) equation

Winn (2010, hereafter W10) proposed an expression for T based on modification to the SMO03 equation. The first change was to modify the impact parameter from $a_R \cos i \rightarrow \varrho_c a_R \cos i$, i.e. to allow for the altered planet–star separation for eccentric orbits. Secondly, the altered planetary velocity should also be incorporated. W10 propose that a reasonable approximation for the transit duration is obtained by multiplying the SMO03 expressions by the following ratio:

$$\frac{(dX/dt)(f_c)[e=0]}{(dX/dt)(f_c)} = \frac{\varrho_c}{\sqrt{1 - e^2}}, \quad (24)$$

where X is given in W10 and f_c is the true anomaly at the centre of the transit. This yields a new transit duration equation of

$$T_{\text{W10}} = \frac{P}{\pi} \frac{\varrho_c}{\sqrt{1 - e^2}} \arcsin \left(\frac{1}{a_R} \left[\frac{1 - a_R^2 \varrho_c^2 \cos^2 i}{\sin^2 i} \right]^{1/2} \right). \quad (25)$$

First, we note an obvious improvement of the W10 expression is that we recover the original SMO03 equation for $e = 0$. Secondly, comparison to the equation for T_1 reveals that the two expressions are very similar except for the position of an extra ϱ_c term. Indeed, the T_1 and T_{W10} expressions are equivalent in the small-angle approximation.

4 NUMERICAL INVESTIGATIONS

4.1 Example systems

Insights into the robustness and accuracy of the various expressions may be obtained through numerical tests of the various approximate expressions. We here compare the accuracy of four expressions: T_{TS05} , T_{W10} , T_1 and T_2 . These expressions depend only on five parameters P , a/R_* , b , $e \sin \omega$ and $e \cos \omega$. One of the clearest ways of visually comparing the equations is to consider a typical transiting exoplanet example with system parameters for a/R_* and b and vary the eccentricity parameters. P may be selected by simply assuming a star of solar density.

We create a 1000×1000 grid of $e \sin \omega$ and $e \cos \omega$ values from -1 to 1 in equal steps. Grid positions for hyperbolic orbits ($e > 1$) are excluded. We then calculate the transit duration through the exact solution of the quartic equation, T_{K08} , plus all four approximate formulae. We then calculate the fractional deviation of each equation from the true solution using

$$\mathcal{D}_{\text{candidate}} = \frac{T_{\text{candidate}} - T_{\text{K08}}}{T_{\text{K08}}}. \quad (26)$$

We then plot the loci of points for which the deviation is less than 1 per cent (i.e. $\mathcal{D}_{\text{candidate}} < 0.01$). In Fig. 2, we show four such plots for different choices of a/R_* and b . The plot reveals several interesting features.

- (i) T_1 consistently yields the largest loci.
- (ii) T_2 is sometimes accurate and sometimes not, supporting the hypothesis that the approximation is not stable.
- (iii) T_{W10} also yields consistently large loci.
- (iv) T_{TS05} consistently yields the smallest loci.

4.2 Additional tests

We briefly discuss additional tests we performed for two sets of 10^7 different hypothetical transiting exoplanet systems: one for eccentricities $0.0 < e < 1.0$ and one for $0.9 < e < 1.0$. In all cases, we randomly generated the system parameters weighted by the transit probability and calculated the deviation of the various formulae.

We found that the T_1 expressions was consistently the most accurate, with the W10 of similar accuracy but higher asymmetry. We therefore find that the results yield an overall preference for the T_1 approximation. We note that authors using the T_{W10} formulation can also expect an extremely good approximation but for the remainder of this paper we will only consider using T_1 for the later derivations. We may define the ‘improvement’ of the T_1 expression relative to the T_{TS05} equation as

$$\mathcal{I}_{T_1} = [(\mathcal{D}_{\text{TS05}}/\mathcal{D}_{T_1}) - 1] 100, \quad (27)$$

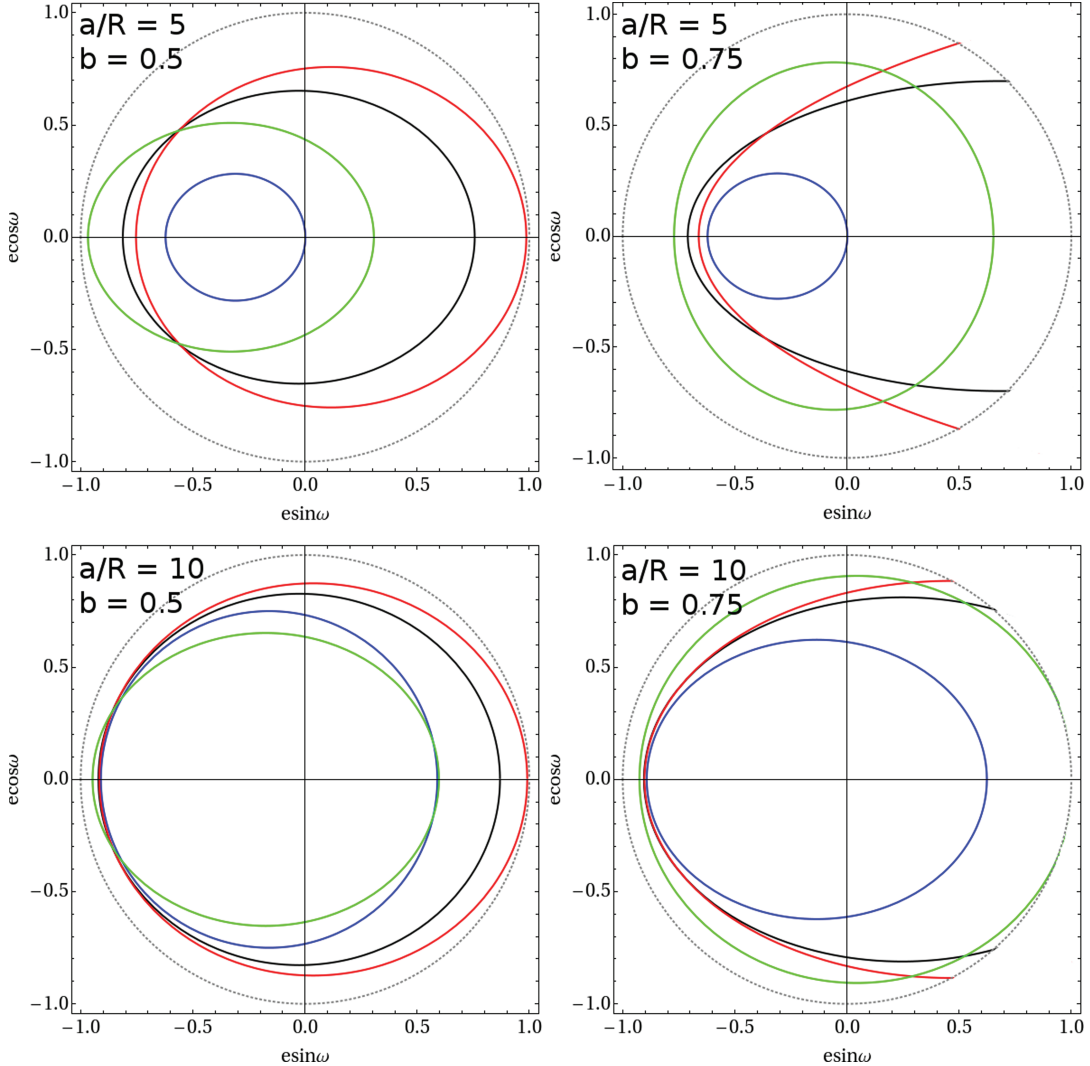


Figure 2. Loci of points for which the accuracy is better than 99 per cent for all four candidate expressions, as a function of eccentricity. The T_1 expression offers both consistency and excellent accuracy. Other system parameters fixed to typical transit values. Blue is for T_{TS05} , black is for T_{W10} , red is for T_1 and green for T_2 . The grey ellipse represents the allowed physical limits.

where \mathcal{I} is measured in per cent. We can see that if TS05 gives a lower deviation (i.e. more accurate solution), we will obtain $\mathcal{I} < 0$ per cent whereas if the candidate expression gives a closer solution we obtain $\mathcal{I} > 0$ per cent and is essentially the percentage improvement in accuracy. For the range $0 < e < 1$, we find the mean value of this parameter is $\mathcal{I}_{T_1} = 210$ per cent, and for the range $< 0.9 < e < 1.0$, we find $\mathcal{I}_{T_1} = 458$ per cent. We note that one caveat of these tests is that they are sensitive to the a priori inputs.

For the case of Kepler photometry, following the method of Kipping, Fossey & Campanella (2009), we estimate that the typical measurement uncertainty on T will be ~ 0.1 per cent in most cases. We find that T_1 is accurate to 0.1 per cent or better over a range of $|e \sin \omega| < 0.5$ and $|e \cos \omega| < 0.85$ on average.

5 ANALYTIC INVESTIGATIONS

5.1 The consequences of using circular expressions for eccentric orbits

SMO03 showed that the first to fourth contact duration, t_T , and the second and third contact duration, t_F , may be used to derive a_R , i , b and the stellar density, ρ_* . We here consider how biased these

retrieved parameters would be if we used the circular equations for an eccentric orbit. From here, we will employ the T_1 expression for the transit duration, as this equation has been shown to provide the greatest accuracy in the previous section. According to SMO03 the circular transit durations are given by

$$t_T(\text{SMO03}) = \frac{P}{\pi} \arcsin \left(\frac{\sqrt{(1+p)^2 - a_R^2 \cos^2 i}}{a_R \sin i} \right), \quad (28)$$

$$t_F(\text{SMO03}) = \frac{P}{\pi} \arcsin \left(\frac{\sqrt{(1-p)^2 - a_R^2 \cos^2 i}}{a_R \sin i} \right). \quad (29)$$

Modification of the T_1 solution gives

$$t_{T,1} = \frac{P}{\pi} \frac{\varrho_c^2}{\sqrt{1-e^2}} \arcsin \left(\frac{\sqrt{(1+p)^2 - a_R^2 \varrho_c^2 \cos^2 i}}{a_R \varrho_c \sin i} \right), \quad (30)$$

$$t_{F,1} = \frac{P}{\pi} \frac{\varrho_c^2}{\sqrt{1-e^2}} \arcsin \left(\frac{\sqrt{(1-p)^2 - a_R^2 \varrho_c^2 \cos^2 i}}{a_R \varrho_c \sin i} \right). \quad (31)$$

Using (28) and (29), SMO03 show that the impact parameter may be retrieved by using

$$\begin{aligned} [b_{\text{derived}}(\text{SMO03})]^2 &= \\ &= \frac{(1-p)^2 - [\sin^2(t_F\pi/P)/\sin^2(t_T\pi/P)](1+p)^2}{1 - [\sin^2(t_F\pi/P)/\sin^2(t_T\pi/P)]}. \end{aligned} \quad (32)$$

Using the same equations for an eccentric orbit gives

$$\begin{aligned} [b_{\text{derived}}(\text{SMO03})]^2 &= 1 + p^2 + 2p \\ &\cdot \left(\frac{\sin^2\left[\frac{\varrho_c^2}{\sqrt{1-e^2}} \arcsin\left(\frac{\sqrt{(1-p)^2-b^2}}{a_R \varrho_c \sin i}\right)\right] + \sin^2\left[\frac{\varrho_c^2}{\sqrt{1-e^2}} \arcsin\left(\frac{\sqrt{(1+p)^2-b^2}}{a_R \varrho_c \sin i}\right)\right]}{\sin^2\left[\frac{\varrho_c^2}{\sqrt{1-e^2}} \arcsin\left(\frac{\sqrt{(1-p)^2-b^2}}{a_R \varrho_c \sin i}\right)\right] - \sin^2\left[\frac{\varrho_c^2}{\sqrt{1-e^2}} \arcsin\left(\frac{\sqrt{(1+p)^2-b^2}}{a_R \varrho_c \sin i}\right)\right]} \right), \end{aligned} \quad (33)$$

where it is understood that for terms on the right-hand side with b in them, we are referring to the true impact parameter, $b = a_R \varrho_c \cos i$. We plot this function in the case of $a_R = 10$, $b^2 = 0.5$ and $p = 0.1$ in Fig. 3. Making small-angle approximations, this yields $b_{\text{derived}}^2 \simeq b^2$. However, for larger $e \sin \omega$ and $e \cos \omega$ values, the overall effect is to overestimate b for eccentric orbits.

In addition to the impact parameter, SMO03 proposed that the parameter $a_R = a/R_*$ may be derived using

$$[a_{R,\text{derived}}(\text{SMO03})]^2 = \frac{(1+p)^2 - b_{\text{derived}}^2}{\sin^2(t_T\pi/P)} + b_{\text{derived}}^2. \quad (34)$$

If we use the assumption $b_{\text{derived}} \simeq b$, then this equation yields

$$[a_{R,\text{derived}}(\text{SMO03})]^2 = b^2$$

$$+ ((1+p^2) - b^2) \csc^2 \left[\frac{\varrho_c^2}{\sqrt{1-e^2}} \arcsin \left(\frac{\sqrt{(1+p)^2-b^2}}{a_R \varrho_c \sin i} \right) \right]. \quad (35)$$

With small-angle approximations, we have

$$a_{R,\text{derived}} \simeq a_R \sqrt{\varrho_c^2 \cos^2 i + \frac{(1-e^2) \sin^2 i}{\varrho_c^2}}. \quad (36)$$

The term inside the square root goes to unity for circular orbits, as expected. The deviation in a_R can be seen to become quite significant for eccentric orbits, as seen in Fig. 4 where the exact expression for (34) is plotted. This will have significant consequences for our next parameter, the stellar density. Stellar density is related to a_R by

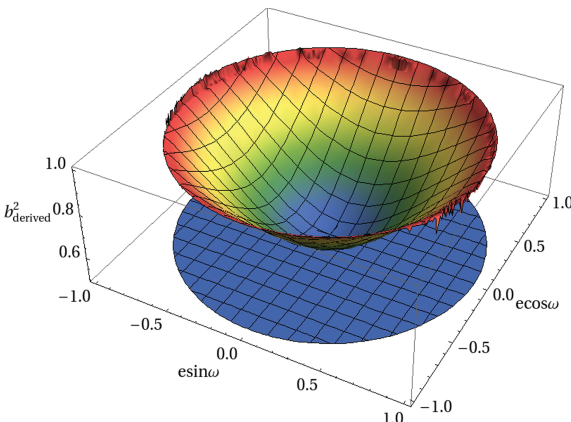


Figure 3. If one uses the circular expressions, the retrieved impact parameter (squared) is heavily biased by eccentricity. In this example, the true value of b^2 is 0.5 but the introduction of eccentricity causes b^2 to be overestimated.

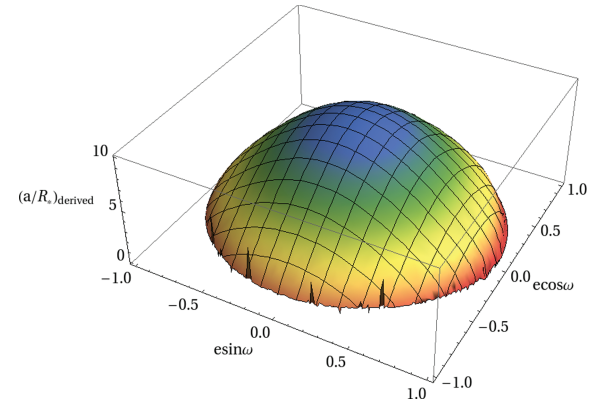


Figure 4. If one uses the circular expressions, the retrieved value of a/R_* is heavily biased by eccentricity. In this example, the true value of a/R_* is 10 but the introduction of eccentricity causes a/R_* to be underestimated.

manipulation of Kepler's laws:

$$\begin{aligned} \rho_* + p^3 \rho_p &= \frac{3\pi}{GP^2} a_R^3, \\ \rho_* &\simeq \frac{3\pi}{GP^2} a_R^3, \end{aligned} \quad (37)$$

where the approximation is made using the assumption $p \ll 1$. We can therefore see that

$$\rho_{*,\text{derived}} \simeq \rho_* \left[\varrho_c^2 \cos^2 i + \frac{(1-e^2) \sin^2 i}{\varrho_c^2} \right]^{3/2}, \quad (38)$$

$$\rho_{*,\text{derived}} \simeq \rho_* \Psi = \left[\frac{(1+e \sin \omega)^3}{(1-e^2)^{3/2}} \right] \rho_*, \quad (39)$$

where in the second line we have assumed that $i \simeq \pi/2$. A series expansion of Ψ into first order of e yields $\Psi \simeq 1 + 3e \sin \omega + \mathcal{O}(e^2)$. So observers neglecting an eccentricity of $e \sim 0.1$ may alter the stellar density by 30 per cent. As an example, if we decreased the density of a solar-type G2V star by 30 per cent, the biased average stellar density would be more consistent with a star of spectral type K0V. Indeed, asteroseismologically determined stellar densities of transiting systems could be used to infer Ψ .

This density bias, which is plotted in Fig. 5, could be extremely crucial in the search for transiting planets. Many discovery papers of new transiting planets have only sparse radial velocity data and

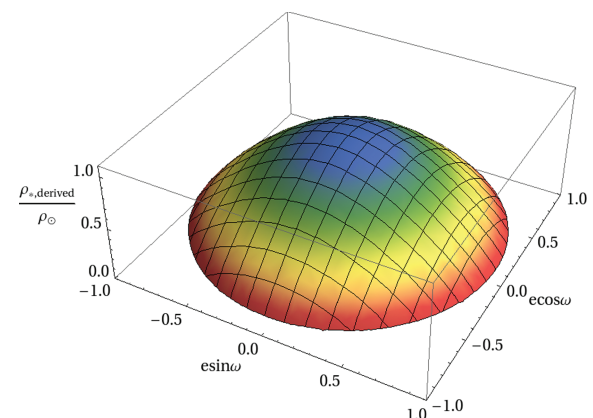


Figure 5. If one uses the circular expressions, the retrieved value of ρ_* is heavily biased by eccentricity. In this example, the true value of ρ_* is $1 \rho_\odot$ but the introduction of eccentricity causes ρ_* to be underestimated.

usually no secondary eclipse measurement. As a result, the uncertainty on the eccentricity is very large.

Critically, planets are often accepted or rejected as being genuine or not on the basis of this light-curve derived stellar density. If the light-curve derived stellar density is very different from the combination of stellar evolution and spectroscopic determination, these candidates are generally regarded as unphysical. This method of discriminating between genuine planets and blends, which may mimic such objects, was proposed by SMO03 (see section 6.3 of SMO03) but crucially only for circular orbits.

Since the typical upper limit on e is around 0.1 in discovery papers, then the light-curve derived stellar density also has a maximum possible error of ~ 30 per cent. In practice, the uncertainty on e will result in a larger uncertainty in ρ_* . Typical procedure is to fix $e = 0$ if the radial velocity data is quite poor, despite the fact the upper limit on $e \sim 0.1$. As a result, the posterior distribution of ρ_* would be artificially narrow and erroneous if $e \neq 0$. We propose that global fits should allow e to vary when analysing radial velocity and transit photometry, as well as a fixed $e = 0$ fit for comparison. This would allow the full range of possible eccentricities to be explored, which would result in a broader and more accurate distribution for b , a_R and critically ρ_* .

5.2 General solution for the physical parameters

In the previous subsection we saw how using the circular expressions to derive a_R and ρ_* can lead to severe errors for even mildly eccentric systems. We here present expressions which will recover excellent approximations values for b , a_R and ρ_* . The new equations are given by

$$b^2 = \frac{(1-p)^2 - \frac{\sin^2\left[\left(t_F\pi\sqrt{1-e^2}\right)/(P\varrho_c^2)\right]}{\sin^2\left[\left(t_T\pi\sqrt{1-e^2}\right)/(P\varrho_c^2)\right]}(1+p)^2}{1 - \frac{\sin^2\left[\left(t_F\pi\sqrt{1-e^2}\right)/(P\varrho_c^2)\right]}{\sin^2\left[\left(t_T\pi\sqrt{1-e^2}\right)/(P\varrho_c^2)\right]}}, \quad (40)$$

$$a_R^2 = \frac{(1+p^2)-b^2}{\varrho_c^2 \sin^2[(t_T\pi\sqrt{1-e^2})/(P\varrho_c^2)]} + \frac{b^2}{\varrho_c^2}, \quad (41)$$

$$\rho_* = \frac{3\pi}{GP^2} a_R^3 - p^3 \rho_p. \quad (42)$$

These expressions can be shown to reduce down to the original SMO03 derivations if $e \rightarrow 0$ (equations 7 and 8 of SMO03). The new stellar density parameter may be used with floating e and ω values to correctly estimate the probability distribution of this critical parameter.

5.3 The transit ‘width’ duration

In the previous subsection, we have derived the physical parameters in terms of t_T and t_F . We may naively assume that this is interchangeable with expressions in terms of T and τ . Assuming the transit light curve is symmetric (exactly valid for circular orbits and a very good approximation for eccentric orbits), the following relations between these two definitions exist:

$$\tau = \frac{t_T - t_F}{2}, \quad (43)$$

$$T \neq \frac{t_T + t_F}{2} = W. \quad (44)$$

For the latter, $T = W$ for the trapezoid approximated light curve only. This is because T is defined as when the sky-projection of the planet’s centre is touching the stellar limb, i.e. $S = 1$. At this point, the fraction of the planetary disc occulting the stellar disc is not equal to one half of the total in-transit occulted area. In contrast, we here define W as the duration between the midway of the ingress to the midway of the egress. We can intuitively see at the moment $S = 1$, less than half of the total area must be occulted and therefore $T > W = (t_T + t_F)/2$.

A further validation of this can be seen by writing down the equations for t_T and t_F and combining them using arcsin trigometric identities. For the simple case of a circular orbit, the resultant expression would give

$$W(e=0) = \frac{P}{\pi} \arcsin\left(\frac{\sqrt{1-\sqrt{1-\alpha^2}}}{\sqrt{2}}\right), \quad (45)$$

$$\alpha = (a_R \sin i)^{-1} [(1+p)^2 - b^2]^{1/2} [1 - (1-p^2) + b^2]^{1/2} - [(1-p)^2 - b^2]^{1/2} [1 - (1+p^2) + b^2]^{1/2}. \quad (46)$$

It may be shown that $\alpha \neq \sqrt{1-b^2}/(a_R \sin i)$ and thus $W \neq T$. In the same manner as we derived W , τ may also be written as a combination of the relevant arcsin functions. However, we can already see that such an expression will also be extremely laborious. This means that writing down the expressions for $b(T, \tau)$ and $a_R(T, \tau)$ is much more challenging than that for $b(t_T, t_F)$ and $a_R(t_T, t_F)$ and we were unable to find an exact inversion relation. Indeed, finding exact expressions for these inverse relations is unnecessary as we may retrieve b and a_R using equations (40) and (41).

For a circular orbit and in the limit $a_R \gg 1$, the relative difference between T and W may be written as

$$\frac{T_1 - W_1}{T_1} \sim \frac{2\sqrt{1-b^2} - \sqrt{(1+p)^2 - b^2} - \sqrt{(1-p)^2 - b^2}}{2\sqrt{1-b^2}}. \quad (47)$$

Notice how for $p \rightarrow 0$ this expression yields zero, which is expected since the planet now takes infinitesimal size. The denominator also reveals that the difference diverges rapidly for near-grazing transits, i.e. $b \rightarrow 1$.

6 APPLICATIONS TO LIGHT-CURVE FITTING

6.1 Fitting parameter sets: $\{t_c, p^2, W_1, \tau_1\}$

The transit light curve is essentially described by four physical parameters, which form the parameter set $\{t_c, p, a_R, b\}$. However, efforts to fit transit light curves using this parameter set is known to be highly inefficient due to large interparameter correlations, in particular between a_R and b . Carter et al. (2008) used a Fisher analysis to show that for a symmetric light curve, which is approximated as a piece-wise linear model (i.e. a trapezoid), a superior parameter set to fit for is given by $\{t_c, p^2, T, \tau\}$, where τ is the ingress or equivalently egress duration assuming a symmetric light curve. In our case, these parameters become $\{t_c, p^2, T_1, \tau_1\}$. The authors reported that using this parameter set decreased the correlation lengths in a Markov chain Monte Carlo (MCMC) fit by a factor of ~ 150 .

In the Carter et al. (2008) analysis, the light curve is a symmetric trapezoid and therefore $W = T$. As we have already seen, this is not true for a real light curve. This raises the ambiguity as to whether this fitting parameter should be W or T for real light curves.

One advantage of the T parameter is that it is independent of p , whereas W is not. With one degree less of freedom than W , T

will always exhibit lower correlations and may be determined to lower uncertainty. This makes T ideal for transit duration variations (TDVs) studies, as pointed out by Kipping et al. (2009). However, as we saw in Section 5.3, there presently exists no known expression for converting T and τ into the physical parameter set which is used to actually generate a model light curve.

When fitting a transit light curve, our hypothetical algorithm must make trial guesses for ‘the fitting parameter set’ which is then mapped into ‘the physical parameter set’. These physical parameters are then fed into a transit light-curve model generator, allowing for the goodness-of-fit between the trial model and the observations to be made. This mapping procedure is unavoidable since the transit light curve is essentially generated by feeding the sky-projected planet–star separation, S , as a function of time, into a light-curve generating code like that of Mandel & Agol (2002). Since S (equation 4) is a function of the physical parameter set, and not the fitting parameter set, the mapping between the two sets is a prerequisite for any light-curve fitting algorithm.

Unless an approximation is made that $T_1 \simeq W_1$, there currently exists no expressions which perform this mapping procedure for the fitting parameter set $\{t_c, p^2, T_1, \tau_1\}$.¹ Specifically, there currently exists no exact expression for $b(T_1, \tau_1, p)$ and $a_R(T_1, \tau_1, p)$. Therefore, $\{t_c, p^2, T_1, \tau_1\}$ cannot be used as a fitting parameter set unless we assume $T_1 \simeq W_1$ and use $\{t_c, p^2, W_1, \tau_1\}$.

Fortunately, the consequences of making this assumption will not be severe, in most cases. This is because the trial fitting parameters serve only one function – to produce trial physical parameters. These trial physical parameters may be slightly offset from the exact mapping but this is not particularly crippling since the model light curve is still generated exactly based upon these trial physical parameters. The only negative consequence of using this method is that an additional correlation has been introduced into the fitting algorithm since the offset between T and W will be a function of b and p . This correlation will be largest for near-grazing transits since equation (47) tends towards ∞ as $b \rightarrow 1$. In general, we wish to avoid such correlations as much as possible to allow the algorithm to most efficiently explore the parameter space.

6.2 Fitting parameter sets: $\{t_c, G_1, W_1, A_1\}$

For a trapezoid approximated light curve, Carter et al. (2008) showed that the fitting parameter correlations are decreased further by using the parameter set $\{t_c, G, W, A\}$, where A is the area of the trapezoid-approximated light curve, and G is the gradient of the ingress/egress (note we have changed the original notation from S to G to avoid confusion with equation 4).²

The area of the trapezoid light curve is given by $\delta(t_T + t_F)/2$, where $\delta = p^2$. The gradient of a trapezoid slope is given by δ/τ . Since $\tau = (t_T - t_F)/2$ then both A and G may be written as a function of t_T and t_F only, thus obviating the use of T and the associated issues discussed in the previous subsection.

In order to proceed, a mapping from $\{G, W, A\} \rightarrow \{p, a_R, b\}$ is required for accomplishing this goal. The exact solutions for G , W and A may be found by solving the quartic equation discussed in Section 2. However, the roots of this equation yields $G(p, a_R, b)$,

¹Although mappings have been proposed, they all make the assumption $T = W$.

²We note that Carter et al. (2008) proposed an additional slightly improved parameter set, but this set required reliable prior estimates of b and lacked a physical interpretation.

$W(p, a_R, b)$ and $A(p, a_R, b)$ whereas we need the inverse relations. Since no concise analytic solution for the inverse relations currently exists, these inverse relations would have to be calculated through a numerical iteration but such a process would need to be repeated for every single trial leading to vastly greater computation time for a fitting algorithm.

Therefore, a practical compromise is to use approximate formulae $G_1(p, a_R, b)$, $W_1(p, a_R, b)$ and $A_1(p, a_R, b)$, which are easily manipulated to give the inverse relations: $p(G_1, W_1, A_1)$, $a_R(G_1, W_1, A_1)$ and $b(G_1, W_1, A_1)$.

It is critical to understand that using equations for a circular orbit or an approximate eccentric expression of poor accuracy will cause fitting algorithms to wander into unphysical solutions and/or increase interparameter correlations for planets which are eccentric, near-grazing, very close-in, etc. It is therefore imperative to use a mapping which is as accurate as possible in order to have a robust fitting algorithm. The mappings to convert the trial $\{G_1, W_1, A_1\}$ into the physical parameters $\{p, a_R, b\}$ are given by equations (40) and (41) combined with the following replacements:

$$p = \sqrt{\frac{A_1}{W_1}}, \quad (48)$$

$$t_{T,1} = W_1 + \frac{A_1}{W_1 G_1}, \quad (49)$$

$$t_{F,1} = W_1 - \frac{A_1}{W_1 G_1}. \quad (50)$$

We note that the favoured parameter set derived by Carter et al. (2008) assumed a symmetric light curve which is not strictly true for $e > 0$. However, for an eccentric orbit, the degree of asymmetry between the ingress and egress is known to be very small (K08; W10) and thus may be neglected for the purposes of choosing an ideal fitting parameter set.

6.3 Fitting parameter sets: $\{t_c, p^2, \zeta/R_*, b^2\}$

The two parameter sets proposed so far have both included W_1 . Since we know W_1 is a function of p but T_1 is not, any parameter set using W_1 will likely exhibit larger correlations since there is an extra parameter dependency. However, a parameter set based upon T_1 would have to satisfy the condition that it can be inverse mapped into the physical parameters.

A search through the literature finds just such a parameter set. Bakos et al. (2007) proposed the fitting parameter set $\{t_c, p^2, \zeta/R_*, b^2\}$, where ζ/R_* is defined by

$$\begin{aligned} \frac{\zeta}{R_*} &= \frac{2}{T_{TS05}}, \\ \frac{\zeta}{R_*} &= \frac{2\pi a}{P R_*} \frac{1 + e \sin \omega}{\sqrt{1 - e^2} \sqrt{1 - b^2}}. \end{aligned} \quad (51)$$

ζ/R_* , originally defined by Murray & Dermott (1999), can be seen to be reciprocal of one half of the transit duration as defined by TS05. Unlike the $\{t_c, p^2, T, \tau\}$ parameter set, we do not need to assume $T = W$ to produce an inverse mapping. By using T_{TS05} and b^2 , an exact inverse mapping to the physical parameters is possible which offers significant advantages.

Having satisfied the criteria of being both a decorrelated parameter and inverseable, ζ/R_* would appear to an excellent candidate for light-curve fitting. A further improvement to this parameter is

possible by using the new T_1 approximation for the transit duration. Let us define

$$\begin{aligned} \frac{\Upsilon}{R_*} &= \frac{2}{T_1}, \\ \frac{\Upsilon}{R_*} &= \frac{2\pi}{P} \frac{\sqrt{1-e^2}}{\varrho_c^2} \left[\arcsin \left(\frac{\sqrt{1-a_R^2\varrho_c^2 \cos^2 i}}{a_R \varrho_c \sin i} \right) \right]^{-1}. \end{aligned} \quad (52)$$

The inverse mapping would use the expression

$$a_R^2 = \frac{1-b^2}{\varrho_c^2} \csc^2 \left[\frac{2\pi\sqrt{1-e^2}}{P\varrho_c^2(\Upsilon/R_*)} \right] + \frac{b^2}{\varrho_c^2}. \quad (53)$$

6.4 Circular orbit example

Despite the analytic arguments made so far, the clearest validation of which fitting parameter set to employ may be resolved through numerical simulations. This may be done by considering an example system, generating a light curve, adding noise and then refitting using an MCMC routine which outputs the interparameter correlations. We note that analytic expressions for the covariances may be found through Fisher information analysis through the calculation of the relevant partial derivatives (Pál 2008). However, the equations describing the light curve, as given by Mandel & Agol (2002), are quite elaborate and such an analysis remains outside of the scope of this paper. Currently, there exists no exact Fisher information analysis in the literature to draw upon. Carter et al. (2008) avoided this problem by making a trapezoid approximation of the light curve and then implementing a Fisher analysis. As discussed earlier, this requires that we assume $T = W$, which in itself introduces a host of correlations which would be missed by the Fisher analysis methodology. Therefore, exact numerical testing provides a useful alternative to avoid these issues.

First, we consider a superhot Jupiter on a circular orbit with a planet-star separation of $a_R = 3.5$ from a Sun-like star ($P = 0.76$ d). We choose to consider a near-grazing transit with $b = 0.9$ corresponding to an orbital inclination of 75.1° . The light curve is generated using the Mandel & Agol (2002) algorithm with no limb darkening and 0.25 mmag Gaussian noise over a 30-s cadence. The light curve is then passed on to a MCMC fitting algorithm where we try several different parameter sets:

- (i) $\{t_c, p, a_R, b\}$: the physical parameter set;
- (ii) $\{t_c, p^2, \zeta/R_*, b^2\}$: a suggested light-curve fitting parameter by Bakos et al. (2007), based upon the TS05 duration expressions;
- (iii) $\{t_c, p^2, \Upsilon/R_*, b^2\}$: a modified form of the fitting parameter by Bakos et al. (2007), accounting for the improved approximate expression for T ;
- (iv) $\{t_c, p^2, W_1, \tau_1\}$: a suggested set by Carter et al. (2008), where W_1 and τ_1 are calculated using the expressions presented in this paper;
- (v) $\{t_c, G_1, W_1, A_1\}$: a second suggested set by Carter et al. (2008), where G_1 , W_1 and A_1 are calculated using the expressions presented in this paper.

In the MCMC runs, we set the jump sizes to be equal to $\sim 1\sigma$ uncertainties from a preliminary short run. We then start the MCMC from 5σ s away from the solution for each parameter, and use 500 000 trials with a 100 000 burn-in time. We then compute the cross-correlations between the various parameters in trials which are within $\Delta\chi^2 = 1$ of $\chi^2|_{\text{best}}$ (errors rescaled such that $\chi^2|_{\text{best}}$ equals number of data points minus the degrees of freedom). We calculate the interparameter correlations and construct correlation matrices

for each parameter fitting set. As an example, the correlation matrix for the $\{t_c, p, a_R, b\}$ parameter set is given by

$$\text{Corr}(\{t_c, p, a_R, b\}, \{t_c, p, a_R, b\})$$

$$= \begin{pmatrix} 1 & \text{Corr}(t_c, p) & \text{Corr}(t_c, a_R) & \text{Corr}(t_c, b) \\ \text{Corr}(p, t_c) & 1 & \text{Corr}(p, a_R) & \text{Corr}(p, b) \\ \text{Corr}(a_R, t_c) & \text{Corr}(a_R, p) & 1 & \text{Corr}(a_R, b) \\ \text{Corr}(b, t_c) & \text{Corr}(b, p) & \text{Corr}(p, a_R) & 1 \end{pmatrix}.$$

We then calculate the semiprincipal axes of correlation ellipsoid by diagonalizing the matrices. For a completely optimal parameter set, this diagonalized matrix would be the identity matrix. We quantify the departure of each proposed parameter set from the identity matrix by calculating $\sum_{i=1}^4 |M_{i,i} - 1|$, where M is the diagonalized correlation matrix. We display the results in upper half of Table 1.

The correlations of the physical parameter set are predictably very large, in particular between a_R and b which approaches unity. An inspection of the correlations for the other proposed parameter sets suggests that the modified Bakos et al. (2007) formulation offers the lowest correlations. The effect of modifying ζ/R_* to Υ/R_* produces a clear improvement in the corresponding correlations, as seen in Fig. 6. As a result, the numerical tests support using the modified form of the Bakos et al. (2007) parameter set.

Table 1. For each proposed light-curve fitting parameter set (left-hand column), we calculate the interparameter correlation matrices in the examples of (i) a hypothetical near-grazing hot-Jupiter on a circular orbit, (ii) a system similar to the eccentric planet HD 80606b. We diagonalize the correlation matrices to give M and then quantify the departure from a perfectly optimal parameter set (right-hand column), where it is understood that 0 corresponds to optimal and larger values correspond to greater interparameter correlations.

Parameter set	$\sum_{i=1}^4 M_{i,i} - 1 $
Circular orbit example	
$\{t_c, p, a_R, b\}$	2.19333
$\{t_c, p^2, \zeta/R_*, b^2\}$	1.71236
$\{t_c, p^2, \Upsilon/R_*, b^2\}$	1.32974
$\{t_c, p^2, W_1, \tau_1\}$	1.67485
$\{t_c, G_1, W_1, A_1\}$	2.23820
Eccentric orbit example	
$\{t_c, p, a_R, b\}$	2.46676
$\{t_c, p^2, \zeta/R_*, b^2\}$	1.56816
$\{t_c, p^2, \Upsilon/R_*, b^2\}$	1.56776
$\{t_c, p^2, W_1, \tau_1\}$	1.57730
$\{t_c, G_1, W_1, A_1\}$	2.52948

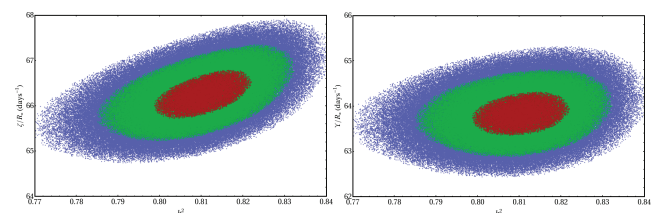


Figure 6. Comparison of the correlations between ζ/R_* vs b^2 (LHS) and Υ/R_* vs b^2 (RHS). Data come from fitting a synthetic hot-Jupiter light curve on a circular, near-grazing orbit with an MCMC algorithm. The new Υ/R_* parameter provides twofold lower correlation and preserves the ability to be inversely mapped to more physical parameters. The three different types of shading represent the 1σ , 2σ and 3σ confidence regions.

6.5 Eccentric orbit example

As a second example, we consider a highly eccentric orbit. In this case, we choose to use the real system HD 80606b. HD 80606b is highly eccentric planet with $e \sim 0.93$ first discovered through radial velocity (Naef et al. 2001) and then later found to go through both secondary and primary eclipse (Fossey, Waldmann & Kipping 2009; Laughlin et al. 2009). Using the system parameters from Winn et al. (2009), we generate a synthetic light curve of cadence 1 min and 1.0 mmag Gaussian noise. We ensure the quantity of out-of-transit baseline data is approximately equal to the full transit duration. We adopt the same methodology as before to calculate the interparameter correlations of the various sets with the results shown in the lower half of Table 1.

In these tests, we find three sets produce approximately the same optimization but the lowest correlations occur for the modified Bakos et al. (2007) set again. The difference between the correlations in the unmodified and the modified Bakos et al. (2007) parameter set is extremely small, but there is a very slight improvement in the modified version. The difference for circular orbits was larger due to the more grazing transit and the fact the TS05 expressions do not reduce down to the circular form. In conclusion, we advocate using the modified Bakos et al. (2007) parameter set, i.e. $\{t_c, p^2, \Upsilon/R_*, b^2\}$ to most efficiently fit transit light curves.

7 SECULAR TRANSIT DURATION VARIATION

TDV can occur two possible formats: (i) periodic change (ii) secular change. As an example, periodic change in the transit duration was predicted to occur for a transiting planet with a companion moon by Kipping (2009a,b). Conceptually analogous to the radial velocity of finding planets, the sky-projected tangential velocity of the planet oscillates around some local mean value as a result of the moon's gravitational tug. These changes in tangential velocity induce variations in the transit duration, allowing for the detection of exomoons as small as $0.2 M_\oplus$ with space-based photometry (Kipping et al. 2009).

Secular changes in transit duration can be caused by numerous possible scenarios. Jordán & Bakos (2008) showed that apsidal precession would induce changes in T and used the TS05 equation to predict the size of these changes. As we have already demonstrated a better formulation for T is possible; we will here present an improved equation for the rate of change in T due to apsidal precession, or essentially changes in ω .

Jordán & Bakos (2008) argued that apsidal precession can be caused by stellar oblateness, general relativistic effects and/or a perturbing planet. Additionally, Murray & Dermott (1999) showed that in general nodal precession should also occur whenever apsidal precession occurs, leading to changes in the orbital inclination angle, i . These changes lead to another form of secular TDV.

Additionally, we consider here that falling planets, such as proposed for WASP-18b (Hellier et al. 2009), would experience a changing semimajor axis, a , leading to another form of secular TDV. Finally, we will consider the effect of varying the orbital eccentricity. All four possible TDVs will be derived here using T_1 , since this expression demonstrated the greatest accuracy in numerical tests.

7.1 Apsidal precession

Apsidal precession is the precession of the argument of periape over time and it may be induced from several different effects including

- (i) general relativistic effects (Einstein 1915; Pál & Kocsis 2008);
- (ii) rotational quadrupole bulges on the planet (Sterne 1939);
- (iii) tides raised on the planet and the star (Sterne 1939);
- (iv) stellar quadrupole moment (Murray & Dermott 1999);
- (v) Kozai mechanism (Kozai 1962);
- (vi) perturbing planets (Murray & Dermott 1999; Miralda-Escudé 2002; Heyl & Gladman 2007).

Out of these examples, planets on nearby orbits of masses $\geq M_\oplus$ are expected to produce the largest effect. Thus the detection of apsidal precession could actually be used to infer the presence of Earth-mass planets.

As Jordán & Bakos (2008) noted, apsidal precession should cause a change in the transit duration and in order to estimate the magnitude of this effect, the authors differentiated T_{TS05} with respect to ω . Having shown the T_1 offers substantial improvement over the T_{TS05} in the previous section, we are here able to provide an improved estimate for the secular TDV caused by apsidal precession:

$$\frac{\partial T}{\partial \omega} = \frac{P}{\pi} \frac{e \varrho_c^3 \cos \omega}{(1 - e^2)^{3/2}} \left(\frac{1}{\sqrt{1 - b^2} \sqrt{a_R^2 \varrho_c^2 - 1}} - 2 \arcsin \left(\frac{\sqrt{1 - b^2}}{a_R \varrho_c \sin i} \right) \right). \quad (54)$$

We can see that there are two terms counteracting in our derived quantity. The two terms can be understood to originate from the planet-star separation changing as a result of the precession which has two effects: (1) decreasing the planet-star separation causes a near-grazing transit's impact parameter to decrease and thus increases T (the first term); (2) decreasing the planet-star separation causes the tangential orbital velocity to increase and thus decreases T (the second term). The $\cos \omega$ term outside of the brackets determines the sign of which term causes an increase and which to decrease.

Kopal (1959) showed that the two effects approximately cancel out for $b \simeq 1/\sqrt{2}$. The Kopal (1959) derivation is quite different for the ones produced in this paper. It is done by first solving for the mid-eclipse time by a series expansion of the differential of the planet-star separation with respect to true anomaly, disregarding terms in $\sin^3 i$ or higher. The duration between the primary and secondary occultation is then solved for in another series expansion in first order of e . Nevertheless, setting b to this value, the terms inside the bracket of equation (54) become

$$\frac{\sqrt{2}}{\sqrt{a_R^2 \varrho_c^2 - 1}} - 2 \arcsin \left(\frac{1}{\sqrt{2} \sqrt{a_R^2 \varrho_c^2 - (1/2)}} \right). \quad (55)$$

Under the condition $a \gg R_*$, we find that equation (54) gives $\partial T / \partial \omega = 0$, in agreement with Kopal (1959). For very close-in orbits, this does not appear to hold.

We may compare our estimate of the apsidal precession to equation (15) of Jordán & Bakos (2008), which was found by differentiating the expression of TS05 with respect to ω . The difference between the two expressions is typically less than 1 per cent across a broad range of parameters. However, if $b \simeq 1/\sqrt{2}$, the difference between the two diverges and can reach 10–100 per cent. Given the sensitivity of both equations to this critical value of b , we recommend numerical calculations over analytic approximations if b is known to be close to 0.707.

7.2 Nodal precession

Nodal precession causes changes in the orbital inclination of the planetary orbit, which would be a source of secular TDV. The secular theory of Murray & Dermott (1999) predicts the rate of inclination change due to a perturbing planet as the nodes precess:

$$\frac{\partial i}{\partial t} = -\frac{\partial \omega}{\partial t} \Delta\Omega_{\text{sky}}, \quad (56)$$

where $\Delta\Omega_{\text{sky}}$ is the ascending node of the perturbing planet relative to the ascending node of the transiting planet, measured clockwise on the plane of the sky. Thus any occurrence of apsidal precession from a perturbing planet will, in general, be coupled with nodal precession. We may derive the rate of secular TDV from inclination change as before and find

$$\frac{\partial T}{\partial i} = \frac{P}{\pi} \frac{\varrho_c^2 \sqrt{a_R^2 \varrho_c^2 - 1}}{\tan i \sqrt{1 - e^2} \sqrt{1 - b^2}}. \quad (57)$$

This expression has only one term and therefore we can see that decreasing the inclination towards a more grazing transit always yields a shorter transit duration, and vice versa.

7.3 Falling exoplanets

Planetary bodies experience infall towards the host star through tidal dissipation and to a much lesser degree gravitational radiation. The effects increase as the orbit becomes smaller leading to runaway fall-in. Therefore, for very close-in exoplanets, the change in semimajor axis may be detectable. The transit duration will vary as

$$\frac{\partial T}{\partial a} = \frac{P}{\pi} \frac{\varrho_c^2}{a \sqrt{1 - e^2}} \left(\frac{3}{2} \arcsin \left(\frac{\sqrt{1 - b^2}}{a_R \varrho_c \sin i} \right) - \frac{1}{\sqrt{1 - b^2} \sqrt{a_R^2 \varrho_c^2 - 1}} \right). \quad (58)$$

As for apsidal precession, there are two counteracting components which are the same as before except for a slightly different constant in front of the first term. This different constant means that the impact parameter at which both effects cancel has now changed to $b \simeq 1/\sqrt{3} = 0.577$. This result could not be found in the previous literature and is of particular interest given the recent discovery of exoplanets on periods of around a day or less, for example WASP-18b (Hellier et al. 2009) with period of 0.94 d and $b = 0.25$.

7.4 Eccentricity variation

Irregular satellites are known to exchange orbital inclination and eccentricity through the Kozai mechanism, which roughly conserves the value $\cos I \sqrt{1 - e^2}$, where I is the angle to the ecliptic. Changes in orbital eccentricity are predicted to lead to long-term transit time variations (L-TTV) by K08, but here we consider the effect on the transit duration too:

$$\frac{\partial T}{\partial e} = \frac{P}{\pi} \frac{\varrho^3}{(1 - e^2)^{5/2}} \left[\frac{2e + (1 + e^2) \sin \omega}{\sqrt{1 - b^2} \sqrt{a_R^2 \varrho_c^2 - 1}} - [3e + (2 + e^2) \sin \omega] \arcsin \left(\frac{\sqrt{1 - b^2}}{a_R \varrho_c \sin i} \right) \right]. \quad (59)$$

The two terms here seem to exhibit a more complicated interdependency which is physically based on the same idea of varying the planet-star separation. The balance point between the two effects

occurs for

$$b \simeq \sqrt{\frac{e + \sin \omega}{(3e + (2 + e^2) \sin \omega)}}. \quad (60)$$

8 CONCLUSIONS

We have derived and tested a new approximate expression for the transit duration of an extrasolar planet with non-zero orbital eccentricity (equation 15). The expression has been shown to analytically reduce down to the exact expressions for a circular orbit, unlike the most previously utilized equation. In numerical tests, the new equation is shown to be more accurate than the other candidate expressions considered in this work, in particular for highly eccentric systems. Quantitatively, the new expression yields a >200 per cent improvement in accuracy over the previously most utilized expression.

Manipulation of the new expression provides for a new light-curve fitting parameter set which is based upon a modification of a previously proposed set by Bakos et al. (2007). The new parameter set is shown to demonstrate the lowest mutual correlations compared to other most commonly used parameter sets and therefore yields the most efficient algorithm for fitting light curves.

Additionally, we have shown that the effect of even mild eccentricity can cause very large biases in the light-curve derived stellar density, which is often used a method for discriminating between planets and blends in transit surveys. Consequently, planetary candidates can be either falsely rejected or accepted for systems with poor constraints on the eccentricity.

Finally, we have used the new equation to derive the rates of secular TDV as a result of apsidal precession, nodal precession (e.g. due to a perturbing planet), in-falling extrasolar planets and eccentricity variation (e.g. Kozai mechanism). These derivatives will provide for a more accurate interpretation of secular TDV.

ACKNOWLEDGMENTS

DMK has been supported by HAT-NET and HAT-South, the Harvard-Smithsonian Center for Astrophysics pre-doctoral fellowships and the Science Technology and Facilities Council (STFC) studentships. Author is grateful to A. Pál for extremely helpful comments which improved the quality of this manuscript. Special thanks to G. Bakos for thought-provoking discussions on the subject. Thanks to G. Bakos and G. Tinetti for their continued support and advice.

REFERENCES

- Bakos G. Á. et al., 2007, ApJ, 670, 826
- Carter J. A., Yee J. C., Eastman J., Gaudi B. S., Winn J. N., 2008, ApJ, 689, 499
- Einstein A., 1915, Preuss. Akad. Wiss. Berlin, 47, 831
- Ford E. B., Quinn S. N., Veras D., 2008, ApJ, 678, 1407
- Fossey S., Waldmann I., Kipping D., 2009, MNRAS, 396, 16
- Hellier C. et al., 2009, Nat, 460, 1098
- Heyl J. S., Gladman B. J., 2007, MNRAS, 377, 1511
- Jordán A., Bakos G. Á., 2008, ApJ, 685, 543
- Kipping D. M., 2008, MNRAS, 389, 1383 (K08)
- Kipping D. M., 2009a, MNRAS, 392, 181
- Kipping D. M., 2009b, MNRAS, 396, 1797
- Kipping D. M., Tinetti G., 2010, ApJ, accepted

- Kipping D. M., Fossey S. J., Campanella G., 2009, MNRAS, 400, 398
 Kopal Z., 1959, Close Binary Systems. Chapman & Hall, London
 Kozai Y., 1962, AJ, 67, 591
 Laughlin G., Deming D., Langton J., Kasen D., Vogt S., Butler P., Rivera E., 2009, Nat, 457, 562
 Mandel K., Agol E., 2002, ApJ, 580, L171
 Miralda-Escudé J., 2002, ApJ, 564, 1019
 Murray C. D., Dermott S. F., 1999, Solar System Dynamics. Cambridge Univ. Press, Cambridge
 Naef D. et al., 2001, A&A, 375, 37
 Pál A., 2008, MNRAS, 390, 281
 Pál A., Kocsis B., 2008, MNRAS, 389, 191
 Seager S., Hui L., 2002, ApJ, 572, 540
 Seager S., Mallén-Ornelas G., 2003, ApJ, 585, 1038 (SMO03)
 Sterne T. E., 1939, MNRAS, 99, 451; 1940, Proc. Natl. Acad. Sci. USA, 26, 36
 Tingley B., Sackett P. D., 2005, ApJ, 676, 1011 (TS05)
 Winn J. N., 2010, in Seager S., ed., EXOPLANETS. University of Arizona Press, Tucson (W10)
 Winn J. N. et al., 2009, ApJ, 703, 2091

APPENDIX A:

Table A1. List of important parameters used in this paper.

Parameter	Name	Definition
S	Sky-projected separation	Sky-projected separation of the companion's centre and the host star's centre in units of stellar radii
R_*	Radius of the host star	Radius of the host star
R_p	Radius of the companion	Radius of the companion
p	Ratio of radii	Ratio of the companion's radius to the stellar radius (R_p/R_*)
δ	Geometric depth	The observed transit depth in the absence of limb darkening and blended contamination, equal to p^2 .
t_I	First contact	Instant when $S = 1 + p$ and $dS/dt < 0$
t_{II}	Second contact	Instant when $S = 1 - p$ and $dS/dt < 0$
t_c	Mid-transit time	Instant when $dS/dt = 0$, i.e. inferior conjunction
t_{III}	Third contact	Instant when $S = 1 - p$ and $dS/dt > 0$
t_{IV}	Fourth contact	Instant when $S = 1 + p$ and $dS/dt > 0$
t_T	Total duration	Time for companion to move between contact points I and IV
t_F	Full duration	Time for companion to move between contact points II and III
T	Transit duration	Time for companion to move across the stellar disc with entry and exit conditions defined as $S = 1$
W	Transit width	Mean value of t_T and t_F
t_{12}	Ingress duration	Time for companion to move between contact points 1 and 2
t_{34}	Egress duration	Time for companion to move between contact points 3 and 4
τ	Ingress/egress duration	For circular orbits, $t_{12} = t_{34} = \tau$
T_1	T_1 duration	A one-term expression for T derived in this work
T_2	T_2 duration	A two-term expression for T derived in this work
T_{TS05}	TS05 duration	Expression for T derived by Tingley & Sackett (2005)
T_{W10}	W10 duration	Expression for T derived by Winn (2010)
T_{SMO03}	SMO03 duration	Expression for T derived by Seager & Mallén-Ornelas (2003)
f	True anomaly	True anomaly of the companion during its orbit around the host star
E	Eccentric anomaly	Eccentric anomaly of the companion during its orbit around the host star
M	Mean anomaly	Mean anomaly of the companion during its orbit around the host star
μ	Reduced mass	Reduced mass of the companion-star system
J	Angular momentum	Angular momentum of the companion
a	Semimajor axis	Semimajor axis of the companion's orbit
a_R	Semimajor axis	Semimajor axis of the companion's orbit in units of stellar radii
e	Eccentricity	Orbital eccentricity of the companion's orbit
Ω	Longitude of the ascending node	Longitude of the ascending node of the companion's orbit
ϖ	Longitude of pericentre	Longitude of pericentre of the companion's orbit
ω	Argument of pericentre	Argument of pericentre of the companion's orbit ($\omega = \varpi - \Omega$)
q	Companion-star separation	Companion-star separation in units of stellar radii
q_c	Mid companion-star separation	Companion-star separation in units of stellar radii at the moment of mid-transit
P	Period	Orbital period of the companion
b	Impact parameter	Value of S when $dS/dt = 0$
i	Inclination	Orbital inclination of the companion's orbit relative to the line-of-sight of the observer
D	Duration function	A parameter defined by K08
f_a	True anomaly 'a'	The true anomaly of the companion when $S = 1$ and $dS/dt < 0$
f_b	True anomaly 'b'	The true anomaly of the companion when $S = 1$ and $dS/dt > 0$
f_c	Mid-transit true anomaly	The true anomaly of the companion when $dS/dt = 0$

Table A1 – *continued*

Parameter	Name	Definition
f_M	Mean transit true anomaly	Mean of f_b and f_a
f_H	Half true anomalistic duration	One half of the difference between f_b and f_a
E_a	Eccentric anomaly ‘a’	The eccentric anomaly of the companion when $S = 1$ and $dS/dt < 0$
E_b	Eccentric anomaly ‘b’	The eccentric anomaly of the companion when $S = 1$ and $dS/dt > 0$
E_M	Mean transit eccentric anomaly	Mean of E_b and E_a
E_H	Half eccentric anomalistic duration	One half of the difference between E_b and E_a
ρ^*	Stellar density	Average density of the host star
ζ/R^*	Zeta over R^*	The reciprocal of one half of the T_{TS05} duration.
Υ/R^*	Upsilon over R^*	The reciprocal of one half of the T_1 duration
\mathcal{D}	Deviation	Deviation of a candidate duration expression from the exact solution
\mathcal{I}	Improvement	Improvement of a candidate duration expression over the T_{TS05} expression

This paper has been typeset from a $\text{\TeX}/\text{\LaTeX}$ file prepared by the author.